


Configurable Phase Transitions in a Topological Thermal Material

Guoqiang Xu,¹ Ying Li,^{2,3} Wei Li⁴,,⁴ Shanhui Fan,⁵ and Cheng-Wei Qiu^{1,*}

¹*Department of Electrical and Computer Engineering, National University of Singapore, Kent Ridge 117583, Republic of Singapore*

²*Interdisciplinary Center for Quantum Information, State Key Laboratory of Modern Optical Instrumentation, ZJU-Hangzhou Global Scientific and Technological Innovation Center, Zhejiang University, Hangzhou 310027, China*

³*International Joint Innovation Center, Key Lab. of Advanced Micro/Nano Electronic Devices & Smart Systems of Zhejiang, The Electromagnetics Academy at Zhejiang University, Zhejiang University, Haining 314400, China*

⁴*GPL Photonics Laboratory, State Key Laboratory of Applied Optics, Changchun Institute of Optics, Fine Mechanics and Physics Chinese Academy of Sciences, Changchun 130033, China*

⁵*Department of Electrical Engineering, and Ginzton Laboratory, Stanford University, Stanford, California, 94305, USA*



(Received 3 February 2021; accepted 21 June 2021; published 31 August 2021)

Diffusive nature of thermal transportation fundamentally restricts topological characteristics due to the absence of a sufficient parametric space with complex dimensionalities. Here, we create an orthogonal advection space with two advective pairs to reveal the unexplored topological transitions in thermal material. We demonstrate four types of configurable thermal phases, including the nontrivial dynamic-equilibrium distribution, nonchiral steplike π -phase transition, and another two trivial profiles related to the anti-parity-time symmetry nature. Our findings provide a recipe for realizing a topologically robust thermal system under arbitrary perturbations.

DOI: [10.1103/PhysRevLett.127.105901](https://doi.org/10.1103/PhysRevLett.127.105901)

Topological materials, such as the well-established topological insulators [1–5], have set off a wave of discovering nontrivial phenomena in condensed matter physics. Such a revolution has soon aroused considerable interest in Hermitian systems, and further contributed to the emerging areas of topological photonics and acoustics [6–14]. Owing to the unique characteristics of non-Hermitian systems, intense interests have been raised in exploring non-Hermitian quantum [15–19] and classical wave systems [20–26] to achieve non-Hermitian topological materials in many oscillatory fields. Nevertheless, the thermal diffusion process without native oscillation, is usually perceived impossible to give rise to thermally topological transitions. Though some studies have focused on the topological properties of thermal radiation [27–29], these essentially belong to the category of photonics, since thermal radiation is the emission of electromagnetic waves and can be described by the Helmholtz equation rather than the diffusion function. The realization of thermally topological transition is strongly related to the exploration of non-Hermitian topology in thermal diffusion. Conventionally, nontrivial topology and distinct phase transitions in non-Hermitian system are associated with dynamically encircling a pair of exceptional points (EPs) or a single EP in a large enough parameter space. Some pioneering attempts in oscillatory wave experiments [30–34] usually rely on balancing intrinsic oscillations of the system and the imposed gain or loss [35–38]. By imposing oscillatory dynamics to heat transfer, a positive

EP has been revealed in anti-parity-time (APT) heat transfer [39]. However, such an observation fails to derive the underlying non-Hermitian topology in thermal diffusion, let alone any topological transitions in thermal materials. Unlike other non-Hermitian topology or topological materials for oscillatory wave fields, one cannot find a complex plane with at least two temporal evolution dimensions in conventional thermal systems to exhibit the dynamic EP-pair encircling. Unfortunately, this indispensable condition is fundamentally prohibited by the diffusive nature of thermal diffusion with fixed and positive conductivity and structural parameters.

Here, we report the topologically configurable phase transitions in an artificially structured thermal material, and non-Hermitian topological properties are for the very first time revealed in thermal diffusion by establishing a hybrid thermal system with two EPs and adjustable complex dimensionalities in a synthetic space [40]. The nonchiral EP(s) encircling, initially forbidden by diffusive nature, is realized in thermal diffusion through imposing two pairs of orthogonal advectives. A ubiquitous set of realizing thermally topological properties is demonstrated, while four types of configurable thermal phase transitions with varying quantized invariants are experimentally observed under temporal-evolution parameters. Our work showcases the significance and largely unexplored opportunities in topological physics and topological materials. The results may bring new insights to the manipulation of diffusive transport in general [41–48].

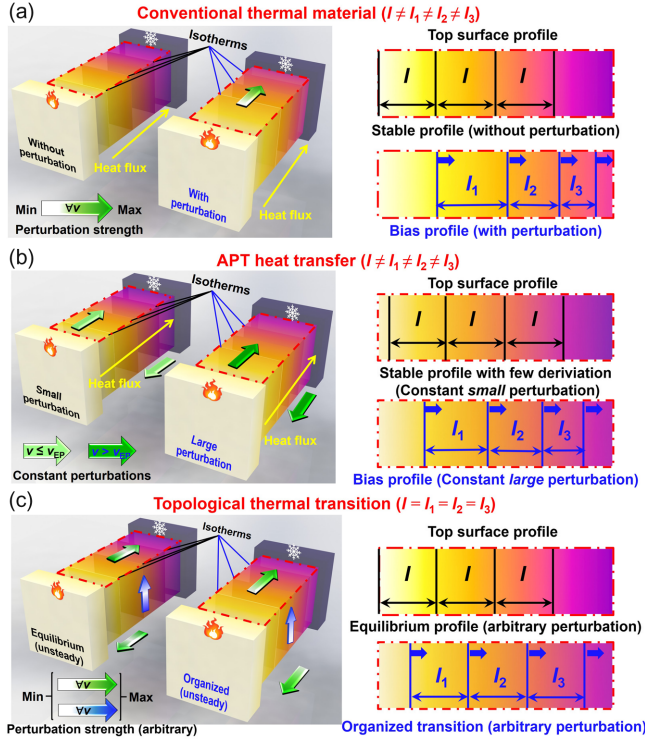


FIG. 1. Contrasts between the conventional and topological thermal structure. The colored plates in the left inserts indicate specific isotherms inside the media, while the black and blue lines are the isotherms on the top surfaces. l denotes equal temperature gap with stable profiles, and $l_1 \sim l_3$ are the ones with dynamic profiles. (a) Conventional thermal material, respectively, under static and perturbed ambient. (b) APT heat transfer under fixed advectations with constant velocities. (c) Topological behavior under arbitrary advectations with changing velocities.

In the beginning, a comparative statement between the conventional and emerging topological thermal structure is provided as shown in Fig. 1. In general, the fixed thermal properties of a conventional thermal system determine the conductive capacity under static ambient. Once external perturbations occur, the thermal distributions would exhibit bias profiles with nonuniform distributions (the isotherms indicated by the blues lines) shown in Fig. 1(a). This is familiar in conventional thermal techniques that are exposed to the convective environments [49,50]. One possible solution is to maintain stable or organized thermal conductivity under convective ambient. Though APT heat transfer [39] seems to be able to keep static temperature profiles under advectations with small constant velocities shown in Fig. 1(b), it remains challenging to satisfy the actual demands with arbitrary velocities. Such problems further provoke a thought: whether an artificially structured thermal system could provide robust or organized conductivity under arbitrarily varying ambient as presented in Fig. 1(c)? The answer could be “yes,” if the robust property of emerging topological materials in oscillatory wave fields could be realized in thermal diffusion under arbitrarily

changing advectations. Hence, the first step is to prove the existence of non-Hermitian topology in thermal diffusion, which is rarely discussed in pure diffusion and intrinsically restricted by the diffusive nature.

Non-Hermitian topology can be realized when the EP pair is completely encircled in a complex plane by multi-adjustable \mathbf{d} vectors [18] or along one complex ($\mathbf{d} + i\lambda_\mu$) vector [19], i.e., $H = I + (\mathbf{d} + i\lambda_\mu)\sigma_\mu$, where μ denotes x , y , z , and \mathbf{d} vector is the real gap vector. Because of the fundamental absence of the complex plane in conventional thermal diffusion, the first step toward realizing non-Hermitian topology in thermal diffusion is to break this natural limitation. We propose an orthogonal conduction-convection framework with two pairs of temporal evolution advectations as the “imitated oscillations” to create an effective complex plane along the vector of $(d_z + i\lambda_z)$ as shown in Fig. 2(a). Here, the counteradvectations on the two lateral sides along the existing heat flux act as the effective “imitated oscillations” in $r - \theta$ plane, while the others on the upper and bottom surfaces offer the effective “imitated oscillations” along the z direction. Thus, the heat transfer process of the motional rings considering the thermal exchanges via conduction through the central medium can be described as

$$\left\{ \begin{array}{l}
 \rho c \frac{\partial T_{1,r\theta}}{\partial t} = \kappa \left(\frac{\partial^2 T_{1,r\theta}}{\partial r^2} + \frac{1}{r} \frac{\partial T_{1,r\theta}}{\partial r} + \frac{\partial^2 T_{1,r\theta}}{\partial \theta^2} \right) + \frac{\rho c v_{1,r\theta}}{r} \frac{\partial T_{1,r\theta}}{\partial \theta} \\
 + \frac{h_{1,r\theta}}{b_{1,r\theta}} (T_{2,r\theta} - T_{1,r\theta}) - \frac{h_{r,z\theta}}{b_{1,r\theta}} (T_{1,z} - T_{1,r\theta}) + \frac{h_{r,z\theta}}{b_{1,r\theta}} (T_{2,z} - T_{1,r\theta}), \\
 \rho c \frac{\partial T_{1,z}}{\partial t} = \kappa \left(\frac{\partial^2 T_{1,z}}{\partial r^2} + \frac{1}{r} \frac{\partial T_{1,z}}{\partial r} + \frac{1}{r^2} \frac{\partial^2 T_{1,z}}{\partial \theta^2} + \frac{\partial^2 T_{1,z}}{\partial z^2} \right) + \rho c v_{1,z} \frac{\partial T_{1,z}}{\partial z} \\
 + \frac{h_{1,z}}{b_{1,z}} (T_{2,z} - T_{1,z}) - \frac{h_{z,r\theta}}{b_{1,z}} (T_{1,r\theta} - T_{1,z}) + \frac{h_{z,r\theta}}{b_{1,z}} (T_{2,r\theta} - T_{1,z}), \\
 \rho c \frac{\partial T_{2,r\theta}}{\partial t} = \kappa \left(\frac{\partial^2 T_{2,r\theta}}{\partial r^2} + \frac{1}{r} \frac{\partial T_{2,r\theta}}{\partial r} + \frac{1}{r^2} \frac{\partial^2 T_{2,r\theta}}{\partial \theta^2} + \frac{\partial^2 T_{2,r\theta}}{\partial z^2} \right) + \frac{\rho c v_{2,r\theta}}{r} \frac{\partial T_{2,r\theta}}{\partial \theta} \\
 + \frac{h_{2,r\theta}}{b_{2,r\theta}} (T_{1,r\theta} - T_{2,r\theta}) + \frac{h_{r,z\theta}}{b_{2,r\theta}} (T_{1,z} - T_{2,r\theta}) - \frac{h_{r,z\theta}}{b_{2,r\theta}} (T_{2,z} - T_{2,r\theta}), \\
 \rho c \frac{\partial T_{2,z}}{\partial t} = \kappa \left(\frac{\partial^2 T_{2,z}}{\partial r^2} + \frac{1}{r} \frac{\partial T_{2,z}}{\partial r} + \frac{1}{r^2} \frac{\partial^2 T_{2,z}}{\partial \theta^2} + \frac{\partial^2 T_{2,z}}{\partial z^2} \right) + \rho c v_{2,z} \frac{\partial T_{2,z}}{\partial z} \\
 + \frac{h_{2,z}}{b_{2,z}} (T_{1,z} - T_{2,z}) + \frac{h_{z,r\theta}}{b_{2,z}} (T_{1,r\theta} - T_{2,z}) - \frac{h_{z,r\theta}}{b_{2,z}} (T_{2,r\theta} - T_{2,z}).
 \end{array} \right. \quad (1)$$

where, ρ , c , and κ are the density, specific heat, and thermal conductivity of the target medium. For the convective components in the $r - \theta$ plane, $T_{1,r\theta}$ and $T_{2,r\theta}$, $b_{1,r\theta}$, and $b_{2,r\theta}$, as well as $v_{1,r\theta}$ and $v_{2,r\theta}$, respectively, denote the temperatures, thicknesses, and velocities of the two lateral layers as indicated in Fig. 2(a). While $h_{1,r\theta}$ and $h_{2,r\theta}$ are the convection heat transfer coefficients of corresponding surfaces. Similarly, $T_{1/2,z}$, $h_{1/2,z}$, $b_{1/2,z}$, $v_{1/2,z}$ are the counterparts for the advective components along the z direction. $h_{r,z\theta}$ and $h_{z,r\theta}$ are the coefficients for the thermal exchanges between the two adjacent rotating and translation rings, respectively, in the $r - \theta$ plane and along the z direction. Three thermal exchanges through the central

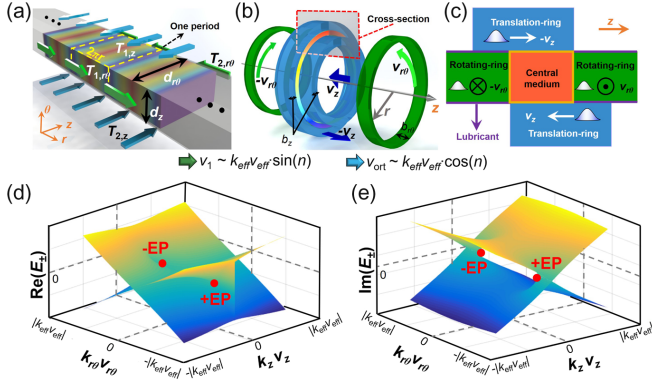


FIG. 2. Realization of the topological transitions in thermal diffusion. (a) Schematic of the topological transitions in thermal diffusion. The green and blue arrows, respectively, denote these advectives with changing velocities in the $r - \theta$ plane and along the z direction, thus forming the orthogonal advective space. One diffusive period, respectively, in the $r - \theta$ plane and along the z direction are highlighted by a yellow dashed border. (b) An achievable multiple ring system coupled with two orthogonal pairs of counterrotational advective components. (c) The cross-section view labeled in the red dashed border of (b). (d) and (e) The complex spectrum in the synthetic parameter space.

medium can be observed between each motional ring and the other three (Supplemental Material [51], Note 2). For simplicity, we make $v_{1,r\theta} = -v_{2,r\theta} = v_{r\theta}$, $v_{1,z} = -v_{2,z} = v_z$, $b_{1,r\theta} = b_{2,r\theta} = b_{1,z} = b_{2,z} = b$, $h_{1,z} = h_{2,z} = h_z$, and $h_{1,r\theta} = h_{2,r\theta} = h_{r,z\theta} = h_{z,r\theta} = h_{r\theta}$.

When the diffusive terms are small enough, each expression can be considered as a one-way wave equation. Then, the temperature profiles would be dominated by the imposed temporal-evolution advectives. That leads to the wavelike periodic temperature distribution in an infinite-long medium as indicated in Fig. 2(a). The diffusive nature makes it hard to achieve periodic convection-conduction in a finite medium along the heat flux. To easily realize such periodic conduction convection, we create a closed-loop ring (radius: r ; perimeter: L) by connecting the two boundaries along the existing heat flux. Thus, an effectively periodic convection-conduction can be obtained with an analog “wave number” $k_{r\theta} = 2\pi n/L = n/r$ around the z direction (n is an integer). Here, we adopt the first mode of $k_{r\theta} = 2\pi/L$ for simplification. For the periodic thermal process along the z direction, we make it repetitively oscillate along the z direction, and denote the thickness of medium layer $d_{1,r\theta}$ as the effective “wavelength” of the imitated “oscillation” indicating an effective wave number $k_z = d_{1,r\theta}^{-1}$. Then, an appropriate system is illustrated in Figs. 2(b) and 2(c). Owing to the geometrical verticality, an orthogonally advective space consisting of two counterrotating advectives in $r - \theta$ plane (green rings) and two countertranslation advectives along the z direction (blue rings) can be achieved around the central medium. In analog to the geometrical meaning of the multiplication

of “ i ,” we introduce such a mathematical operation on the two countertranslation advectives to indicate their orthogonal directions to the ones in $r - \theta$ plane. The effective Hamiltonian can be described as

$$H = i \cdot \begin{bmatrix} - \left(\begin{array}{l} \frac{2\kappa}{\rho c} \cdot (k_{r\theta}^2 + ik_z^2) \\ + \frac{h_{r\theta}}{\rho c b_{r\theta}} + \frac{h_{z,r\theta}}{\rho c b_z} \\ + i \cdot \frac{h_z}{\rho c b_z} + i \cdot \frac{h_{r,z\theta}}{\rho c b_{r\theta}} \end{array} \right) & \frac{h_{r\theta}}{\rho c b_{r\theta}} + \frac{h_{z,r\theta}}{\rho c b_z} \\ & + i \cdot \frac{h_z}{\rho c b_z} + i \cdot \frac{h_{r,z\theta}}{\rho c b_{r\theta}} \\ -i \cdot k_{r\theta} v_{r\theta} - k_z v_z & \\ \frac{h_{r\theta}}{\rho c b_{r\theta}} + \frac{h_{z,r\theta}}{\rho c b_z} & - \left(\begin{array}{l} \frac{2\kappa}{\rho c} \cdot (k_{r\theta}^2 + ik_z^2) \\ + \frac{h_{r\theta}}{\rho c b_{r\theta}} + \frac{h_{z,r\theta}}{\rho c b_z} \\ + i \cdot \frac{h_z}{\rho c b_z} + i \cdot \frac{h_{r,z\theta}}{\rho c b_{r\theta}} \end{array} \right) \\ + i \cdot \frac{h_z}{\rho c b_z} + i \cdot \frac{h_{r,z\theta}}{\rho c b_{r\theta}} & \\ & + i \cdot k_{r\theta} v_{r\theta} + k_z v_z \end{bmatrix}. \quad (2)$$

Because of the much weaker thermal process along the z direction, the related conductive terms and heat exchanges along the z direction can be neglected (Supplemental Material [51], Note 2). Thanks to the orthogonal advective pairs, a complex plane described by a synthetic parameter space $n[k_{\text{eff}} v_{\text{eff}} \cos(n), k_{\text{eff}} v_{\text{eff}} \sin(n)]$ can be obtained, where $n = \arctan(k_{r\theta} v_{r\theta} / k_z v_z)$, and $k_{\text{eff}} v_{\text{eff}} = \sqrt{(k_{r\theta} v_{r\theta})^2 + (k_z v_z)^2}$. Thus, Eq. (2) can be further rewritten as $H = i\{2m\sigma_x - k_{\text{eff}} v_{\text{eff}} [\cos(n) + i \cdot \sin(n)]\sigma_z - [(\kappa/\rho c)k_{r\theta}^2 + 2m]I\}$, $D = \kappa/\rho c$ and $m = (h_{r\theta}/\rho c b_{r\theta}) = (\kappa/\rho c b d_{r\theta}) = (h_{z,r\theta}/\rho c b_z)$. Note that m is fixed and positive for arbitrary thermal systems. The fundamental limitation of diffusive nature is relieved once n sweeps as a function of $k_{\text{eff}} v_{\text{eff}}$, while the underlying non-Hermitian topology can be theoretically anticipated. The complex spectrum in such a synthetic parameter space is shown in Figs. 2(d) and 2(e).

The general non-Hermitian topology and its properties can be evidenced with the dynamic behaviors encircling different quantities of EPs. Here, we select four typical trajectories to validate the existence of non-Hermitian topology in thermal diffusion (Supplemental Material [51], Notes 3 and 4), including (i) one in the region of $|k_{\text{eff}} v_{\text{eff}}| > 2|m|$ encircling two EPs; (ii) one only encircling one EP in the region of $-2|m| < |k_{\text{eff}} v_{\text{eff}}|$ (or $|k_{\text{eff}} v_{\text{eff}}| < 2|m|$); (iii) one without EP in the region of $|k_{\text{eff}} v_{\text{eff}}| < -2|m|$; and (iv) one without EP in the region of $-2|m| < |k_{\text{eff}} v_{\text{eff}}| < 2|m|$. The first and second trajectories, respectively, reveal the $\pm 2\pi$ and $\pm\pi$ geometric phases, while no geometric phase exchanges can be obtained in the third and fourth trajectories without any EPs. The existence of $\pm 2\pi$ geometric phase with the trajectory encircling the EP pair hints the non-Hermitian thermal topology. Then, we further calculate the quantized invariants, including the

eigenstate winding number (ω) and the eigenvalue vorticity (ν). The winding numbers indicate that the integer, half-integer, and zero winding numbers can be theoretically observed with the first, second, and the other trajectories. Note that, the single EP encircling in non-Hermitian optical systems would exhibit chiral transition when the starting point is in the PT-symmetric phase [30–33] and APT-broken phase [34]. Besides, the final states have to stay on the Riemann sheet with gain and nonadiabatic transitions might occur due to the non-Hermiticity, since the oscillatory field propagations on loss sheet are not stable. Hence, one cannot observe the half-integer winding number or the π transition in actual optical experiments [30–34]. In addition, the eigenvalue vorticity defined for the separate bands as the winding number of their energy dispersions also provides similar findings, since the integer, half-integer, and zero vorticities only depend on the quantities of encircling EPs.

We then design a class of thermal systems and elaborate the topologically nontrivial and trivial transitions. The fabricated sample and experimental setups are illustrated in Fig. 3(a). The underlying phase transitions can be identified by the temperature profiles of the surface of central medium and the locations of maximum temperature. Based on the encircling trajectories, we employ four cases

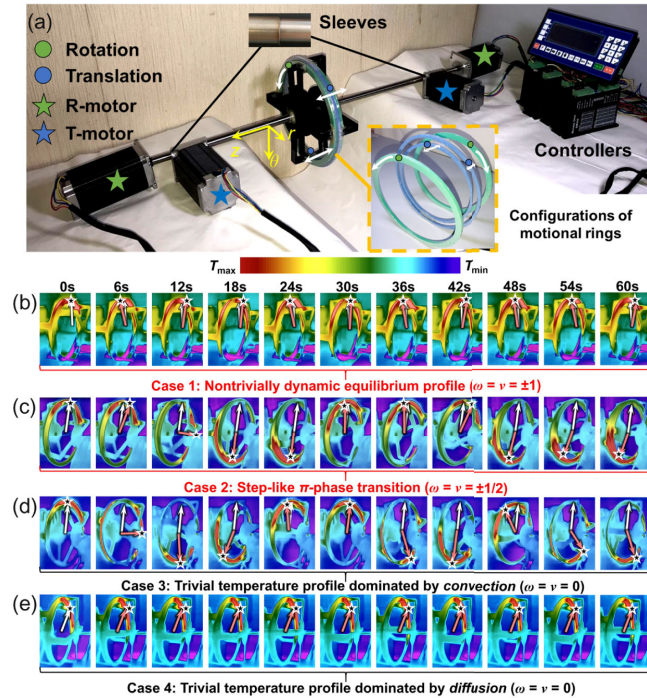


FIG. 3. Experimental setups and captured configurable phase transitions. (a) Experimental setups and fabricated sample. (b)–(e) are the measured profiles of cases 1~4 on the surface of central medium. The black stars imply the T_{\max} locations at specific moments, while the white and red arrows, respectively, denote the initial and measured azimuths. ω and ν denote the winding number and vorticity.

with spatial-temporal advectons, respectively, enclosing different quantities of EPs (Supplemental Material [51], Note 5). The captured temperature profiles of one measured surface are presented in Figs. 3(b)–3(e). While the findings of the other surfaces are shown in Figs. S20–S22 [51].

The topologically nontrivial behavior occurs only when the quantized invariants are integer, and the topologically protected phenomena against the changing advectons are significant in case 1 encircling the EP pair. As shown in Fig. 3(b), S6(a), and S6(b), the temperature profiles at specific moments exhibit a dynamic-equilibrium distribution with respect to the initial one at 0 s, and the changing locations of T_{\max} at specific moments distribute on both sides of its initial location. Such a robustly dynamic-equilibrium phase transition corresponding to the integer quantized invariants enables topologically nontrivial behavior in thermal diffusion. The heat transfer process can now be topologically protected without any bias in temperature profiles.

We then adjust the advective configurations to satisfy case 2 encircling a single EP. Though nontrivial behavior requiring integer quantized invariants cannot be observed in this case, the separate bands of the non-Hermitian system could also provide a distinct state possessing half-integer quantized invariants. As seen in Figs. 3(c), S6(c), and S6(d), the organized dynamic transitions are exhibited during the thermal process, since the temperature profiles remain for a while near the locations of $\theta = n\pi$ when one evolution period is implemented. The temperature profiles thereby present a significant π -phase transition in one period leading to a steplike change as shown in Fig. S6 [51]. Such a steplike π -phase transition is the direct evidence of the π Berry phase and half-integer quantized invariants.

Further removing the EPs from the trajectory, the central medium would act as conventional materials with bias transitions. As illustrated in Fig. 3(d), S6(e), and S6(f), the temperature distributions and T_{\max} locations continuously change towards the advectons during the entire thermal process, resulting in the bias temperature profiles at any time. In contrast, the temperature profiles and T_{\max} locations of case 4 shown in Figs. 3(e), S6(g), and S6(h) almost keep unchanged with tiny perturbations (about 0.002π) to the original state. These transitions are both topologically trivial behaviors in thermal diffusion, which are quite different from the nontrivially dynamic-equilibrium distribution and nonchiral steplike π -phase transition. The magnitudes and relaxation times of T_{\max} for each case are presented in Fig. S5 [51]. Note that, the spatial-temporal advectons might lead to the invalid kinematic similarity, which bring inconvenience in dimensionless thermal analysis (Supplemental Material [51], Note 10). Besides, these behaviors are also robust under different modulated frequency of the advective velocities (Supplemental Material [51], Note 11).

The half-integer winding number and the π -transition can be both observed in case 2, when the starting point is in

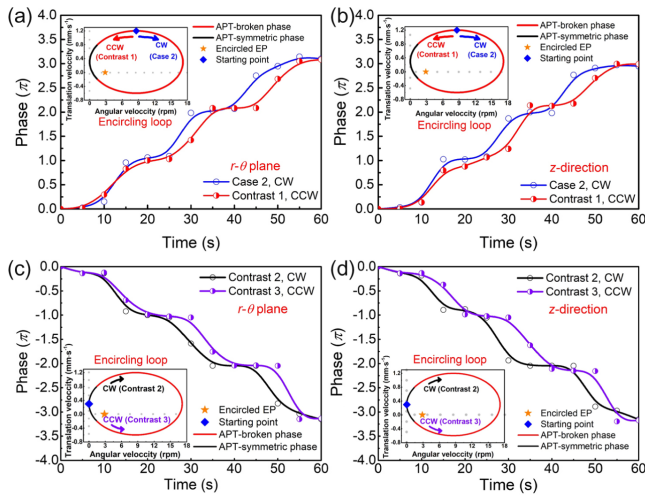


FIG. 4. Nonchiral behaviors of encircling a single EP reflecting on the locations of T_{\max} . The inserts denote the encircling loops while the colored arrows indicate the encircling directions. (a) and (b) The nonchiral behaviors of case 2 (CW) and the contrast 1 (CCW), respectively, in the $r - \theta$ plane and along the z direction, when the starting point is in the APT-broken phase; (c) and (d) Denote the nonchiral behaviors of contrasts 2 (CW) and 3 (CCW), respectively, in the $r - \theta$ plane and along the z direction, when the starting point is in the APT-symmetric phase.

the APT-broken phase. This further leads to the nonchiral dynamics in thermal systems that is independent of the locations of starting point and the encircling directions [counterclockwise (CCW) and clockwise (CW)] as shown in Fig. 4 (Supplemental Material [51], Note 11). Their final states are same whether the starting point is in the APT-broken and APT-symmetric phases, thus revealing the nonchiral encircling in the current thermal system. Furthermore, the transfer directions are opposite if the starting points are in varied phases, i.e., the final states stay on the different sheets.

This phenomenon is distinct from the optical systems exhibiting chiral dynamics [30–34], since the exchanged eigenvectors and half-integer quantized invariant are not usually observed in conventional optical experiments. Such differences can be directly indicated by the target fields, i.e., the diffusive and oscillatory fields. In optical fields, the observed behaviors are based on field oscillations, while loss is the diffusively disturbing term for the entire oscillatory fields. Hence, the oscillatory propagations are decay and unstable with loss (non-Hermiticity), since the inferences of target fields and loss are different. In contrast, thermal diffusion is inherently dissipative and the observed temperature profiles are also dissipations corresponding to the loss terms. The imposed advective processes actually modify the transfer processes, but do not change the propagative nature of diffusion. That is, the inferences of thermal field and non-Hermiticity are consistent and dissipative that allow the hybrid conduction-convection to stably propagate on the loss sheet. That is, nonadiabatic transitions between the

gain and loss sheets in oscillatory fields could be significantly avoided under the continuity of temperature and heat flux in macroscopic thermal system, and the encircling process and final states are available to be realized with loss.

This work proposes a proof-of-concept class of topological transitions in thermal diffusion, via creating a synthetic parameter space in a coupled conduction-advection system with two pairs of orthogonally temporal-evolution advectives. The non-Hermitian topology is first revealed in thermal diffusion, and four types of configurable phase transitions under variant advective configurations are further demonstrated. Among them, the robustly dynamic-equilibrium distribution provides a topologically protected thermal process against the perturbations with changing advective velocities, while the dynamically step-like π -phase transition offers nonchiral thermal diffusion regardless the locations of starting point. None of these transitions can be achieved in conventional thermal materials. The findings pave the way towards creating robust or organized thermal process without bias profiles under unsteady ambient, and immediately stimulate new thoughts for topological thermal sciences as well as other diffusions.

C.-W.Q. acknowledges the financial support of the Ministry of Education, Republic of Singapore (Grant No.: R-263-000-E19-114).

* chengwei.qiu@nus.edu.sg

- [1] L. Fu, C. K. Kane, and E. J. Mele, Topological Insulators in Three Dimensions, *Phys. Rev. Lett.* **98**, 106803 (2007).
- [2] L. Fu and C. K. Kane, Topological insulators with inversion symmetry, *Phys. Rev. B* **76**, 045302 (2007).
- [3] J.E. Moore, The birth of topological insulators, *Nature (London)* **464**, 194 (2010).
- [4] J. Wang and S. C. Zhang, Topological states of condensed matter, *Nat. Mater.* **16**, 1062 (2017).
- [5] N. Xu, Y. Xu, and J. Zhu, Topological insulators for thermoelectrics, *Quantum Mater.* **2**, 51 (2017).
- [6] K. Fang, Z. Yu, and S. Fan, Realizing effective magnetic field for photons by controlling the phase of dynamic modulation, *Nat. Photonics* **6**, 782 (2012).
- [7] G. Harari, M. A. Bandres, Y. Lumer, M. C. Rechtsman, Y. D. Chong, M. Khajavikhan, D. N. Christodoulides, and M. Segev, Topological insulator laser: Theory, *Science* **359**, eaar4003 (2018).
- [8] M. A. Bandres, S. Wittek, G. Harari, M. Parto, J. Ren, M. Segev, D. N. Christodoulides, and M. Khajavikhan, Topological insulator laser: Experiments, *Science* **359**, eaar4005 (2018).
- [9] Y. Lumer and N. Engheta, Topological insulator antenna arrays, *ACS Photonics* **7**, 2244 (2020).
- [10] Z. Zhang, M. H. Teimourpour, J. Arkininstall, M. Pan, P. Miao, H. Schomerus, R. El-Ganainy, and L. Feng, Experimental realization of multiple topological edge states in a 1D photonic lattice, *Laser Photonics Rev.* **13**, 1800202 (2019).

- [11] O. Ilic, I. Kaminer, B. Zhen, O. D. Miller, H. Buljan, and M. Soljacic, Topologically enabled optical nanomotors, *Sci. Adv.* **3**, e1602738 (2017).
- [12] X. Yin, J. Jin, M. Soljacic, C. Peng, and B. Zhen, Observation of topologically enabled unidirectional guided resonances, *Nature (London)* **580**, 467 (2020).
- [13] M. Kim, Z. Jacob, and J. Rho, Recent advances in 2D, 3D and higher-order topological photonics, *Light* **9**, 130 (2020).
- [14] R. Fleury, A. B. Khanikaev, and A. Alu, Floquet topological insulators for sound, *Nat. Commun.* **7**, 11744 (2016).
- [15] W. Hu, H. Wang, P. P. Shum, and Y. D. Chong, Exceptional points in a non-Hermitian topological pump, *Phys. Rev. B* **95**, 184306 (2017).
- [16] Q. Zhong, M. Khajavikhan, D. N. Christodoulides, and R. El-Ganainy, Winding around non-Hermitian singularities, *Nat. Commun.* **9**, 1 (2018).
- [17] H. Shen, B. Zhen, and L. Fu, Topological Band Theory for Non-Hermitian Hamiltonians, *Phys. Rev. Lett.* **120**, 146402 (2018).
- [18] A. Ghatak and T. Das, New topological invariants in non-Hermitian systems, *J. Phys. Condens. Matter* **31**, 263001 (2019).
- [19] D. Leykam, K. Y. Bliokh, C. Huang, Y. D. Chong, and F. Nori, Edge Modes, Degeneracies, and Topological Numbers in Non-Hermitian Systems, *Phys. Rev. Lett.* **118**, 040401 (2017).
- [20] M. Aidelsburger, M. Atala, M. Lohse, J. T. Barreiro, B. Paredes, and I. Bloch, Realization of the Hofstadter Hamiltonian with Ultracold Atoms in Optical Lattices, *Phys. Rev. Lett.* **111**, 185301 (2013).
- [21] Y. Xu, S. T. Wang, and L. M. Duan, Weyl Exceptional Rings in a Three-Dimensional Dissipative Cold Atomic Gas, *Phys. Rev. Lett.* **118**, 045701 (2017).
- [22] W. Chen, S. K. Özdemir, G. Zhao, J. Wiersig, and L. Yang, Exceptional points enhance sensing in an optical microcavity, *Nature (London)* **548**, 192 (2017).
- [23] J. Zhang, B. Peng, S. K. Özdemir, K. Pichler, D. O. Krimer, G. Zhao, F. Nori, Y. Liu, S. Rotter, and L. Yang, A phonon laser operating at an exceptional point, *Nat. Photonics* **12**, 479 (2018).
- [24] B. Midya, H. Zhao, and L. Feng, Non-Hermitian photonics promises exceptional topology of light, *Nat. Commun.* **9**, 2674 (2018).
- [25] H. Zhao, X. Qiao, T. Wu, B. Midya, S. Longhi, and L. Feng, Non-Hermitian topological light steering, *Science* **365**, 1163 (2019).
- [26] A. Cerjan, S. Huang, M. Wang, K. P. Chen, Y. Chong, and M. C. Rechtsman, Experimental realization of a Weyl exceptional ring, *Nat. Photonics* **13**, 623 (2019).
- [27] N. Dahan, Y. Gorodetski, K. Frischwasser, V. Kleiner, and E. Hasman, Geometric Doppler Effect: Spin-Split Dispersion of Thermal Radiation, *Phys. Rev. Lett.* **105**, 136402 (2010).
- [28] T. Eichelkraut, R. Heilmann, S. Weimann, S. Stützer, F. Dreisow, D. N. Christodoulides, S. Nolte, and A. Szameit, Mobility transition from ballistic to diffusive transport in non-Hermitian lattices, *Nat. Commun.* **4**, 2533 (2013).
- [29] P. N. Dyachenko, S. Molesky, A. Y. Petrov, M. Störmer, T. Krekeler, S. Lang, M. Ritter, Z. Jacob, and M. Eich, Controlling thermal emission with refractory epsilon-near-zero metamaterials via topological transitions, *Nat. Commun.* **7**, 11809 (2016).
- [30] J. Doppler, A. A. Mailybaev, J. Böhm, U. Kuhl, A. Girschik, F. Libisch, T. J. Milburn, P. Rabl, N. Moiseyev, and S. Rotter, Dynamically encircling an exceptional point for asymmetric mode switching, *Nature (London)* **537**, 76 (2016).
- [31] H. Xu, D. Mason, L. Jiang, and J. G. E. Harris, Topological energy transfer in an optomechanical system with exceptional points, *Nature (London)* **537**, 80 (2016).
- [32] J. W. Yoon, Y. Choi, C. Hahn, G. Kim, S. K. Song, K. Y. Yang, J. Y. Lee, Y. Kim, C. S. Lee, J. K. Shin, H. S. Lee, and P. Berini, Time-asymmetric loop around an exceptional point over the full optical communications band, *Nature (London)* **562**, 86 (2018).
- [33] X. L. Zhang, S. Wang, B. Hou, and C. T. Chan, Dynamically Encircling Exceptional Points: In Situ Control of Encircling Loops and the R of the Starting Point, *Phys. Rev. X* **8**, 021066 (2018).
- [34] X. Zhang, T. Jiang, and C. T. Chan, Dynamically encircling an exceptional point in anti-parity-time symmetric systems: asymmetric mode switching for symmetry-broken modes, *Light* **8**, 88 (2019).
- [35] S. K. Özdemir, S. Rotter, F. Nori, and L. Yang, Parity-time symmetry and exceptional points in photonics, *Nat. Mater.* **18**, 783 (2019).
- [36] L. Feng, Y. L. Xu, W. S. Fegadolli, M. H. Lu, J. E. B. Oliveira, V. R. Almeida, Y. F. Chen, and A. Scherer, Experimental demonstration of a unidirectional reflectionless parity-time metamaterial at optical frequencies, *Nat. Mater.* **12**, 108 (2013).
- [37] H. Hodaei, M. A. Miri, M. Heinrich, D. N. Christodoulides, and M. Khajavikhan, Parity-time-symmetric microring lasers, *Science* **346**, 975 (2014).
- [38] L. Feng, Z. J. Wong, R. M. Ma, Y. Wang, and X. Zhang, Single-mode laser by parity-time symmetry breaking, *Science* **346**, 972 (2014).
- [39] Y. Li, Y. G. Peng, L. Han, M. A. Miri, W. Li, M. Xiao, X. F. Zhu, J. Zhao, A. Alù, S. Fan, and C. W. Qiu, Anti-parity-time symmetry in diffusive systems, *Science* **364**, 170 (2019).
- [40] L. Yuan, Q. Lin, M. Xiao, and S. Fan, Synthetic dimension in photonics, *Optica* **5**, 1396 (2018).
- [41] P. Dutt, Q. Lin, L. Yuan, M. Minkov, M. Xiao, and S. Fan, A single photonic cavity with two independent physical synthetic dimensions, *Science* **367**, 59 (2020).
- [42] C. Z. Fan, Y. Gao, and J. P. Huang, Shaped graded materials with an apparent negative thermal conductivity, *Appl. Phys. Lett.* **92**, 251907 (2008).
- [43] S. Yang, J. Wang, G. L. Dai, F. B. Yang, and J. P. Huang, Controlling macroscopic heat transfer with thermal metamaterials: Theory, experiment and application, *Phys. Rep.* **908**, 1 (2021).
- [44] J. Zhu, K. Hippalgaonkar, S. Shen, K. Wang, J. Wu, X. Yin, A. Majumdar, and X. Zhang, Temperature-gated thermal rectifier for active heat flow control, *Nano Lett.* **14**, 4867 (2014).
- [45] P. N. Dyachenko, S. Molesky, A. Yu Petrov, M. Störmer, T. Krekeler, S. Lang, M. Ritter, Z. Jacob, and M. Eich, Controlling thermal emission with refractory

- epsilon-near-zero metamaterials via topological transitions, *Nat. Commun.* **7**, 11809 (2016).
- [46] Y. Li, W. Li, T. Han, X. Zheng, J. Li, B. Li, S. Fan, and C. W. Qiu, Transforming heat transfer with thermal metamaterials and devices, *Nat. Rev. Mater.* **6**, 488 (2021).
- [47] G. Xu, K. Dong, Y. Li, H. Li, K. Liu, L. Li, J. Wu, and C. W. Qiu, Tunable analog thermal material, *Nat. Commun.* **11**, 6028 (2020).
- [48] M. Camacho, B. Edwards, and N. Engheta, Achieving asymmetry and trapping in diffusion with spatiotemporal metamaterials, *Nat. Commun.* **11**, 3733 (2020).
- [49] A. P. Raman, M. Abou Anoma, L. Zhu, E. Rephaeli, and S. Fan, Passive radiative cooling below ambient air temperature under direct sunlight, *Nature (London)* **515**, 540 (2014).
- [50] S. Zhuang, L. Zhou, W. Xu, N. Xu, X. Hu, X. Li, G. Lv, Q. Zheng, S. Zhu, Z. Wang, and J. Zhu, Tuning transpiration by interfacial solar absorber-leaf engineering, *Adv. Sci.* **5**, 1700497 (2018).
- [51] See Supplemental Material at <http://link.aps.org/supplemental/10.1103/PhysRevLett.127.105901> for the eigenvalue vorticity (Note 4), which includes Ref. [52]; for the perspective (Note 9), which includes Refs. [53–59], and for the topological descriptions with the non-Hermitian framework (Note 10), which includes Refs. [60–66].
- [52] L. Jin and Z. Song, Bulk-boundary correspondence in a non-Hermitian system in one dimension with chiral inversion symmetry, *Phys. Rev. B* **99**, 081103 (2019).
- [53] Y. Li, K. J. Zhu, Y. G. Peng, W. Li, T. Yang, H. X. Xu, H. Chen, X. F. Zhu, S. Fan, and C. W. Qiu, Thermal meta-device in analogue of zero-index photonics, *Nat. Mater.* **18**, 48 (2019).
- [54] T. Han, J. Zhao, T. Yuan, D. Y. Lei, B. Li, and C. W. Qiu, Theoretical realization of an ultra-efficient thermal-energy harvesting cell made of natural materials, *Energy Environ. Sci.* **6**, 3537 (2013).
- [55] T. Han, X. Bai, D. Gao, J. T. L. Thong, B. Li, and C. W. Qiu, Experimental Demonstration of a Bilayer Thermal Cloak, *Phys. Rev. Lett.* **112**, 054302 (2014).
- [56] Y. Li, X. Bai, T. Yang, H. Luo, and C. W. Qiu, Structured thermal surface for radiative camouflage, *Nat. Commun.* **9**, 273 (2018).
- [57] X. Zhou and G. Xu, Self-adaptive field manipulation with thermal logic material, *Int. J. Heat Mass Transfer* **172**, 121147 (2021).
- [58] N. Doan and N. Swaminathan, Autoignition and flame propagation in non-premixed MILD combustion, *Combust. Flame* **201**, 234 (2019).
- [59] F. Ye, W. Tang, F. Xie, M. Yin, J. He, Y. Wang, H. Chen, Y. Qiang, X. Yang, and L. Han, Low temperature soft cover deposition of uniform large scale perovskite films for high-performance solar cells, *Adv. Mater.* **29**, 1701440 (2017).
- [60] J. Kunes, *Dimensionless Physical Quantities in Science and Engineering* (Elsevier, New York, 2012).
- [61] A. G. Atkins and M. P. Escudier, *A Dictionary of Mechanical Engineering*, (Oxford University Press, New York, 2013), p. 247.
- [62] Y. A. Çengel and J. M. Cimbala, *Fluid Mechanics: Fundamentals and Applications* (McGraw Hill Boston, MA, 2010), p. 300.
- [63] B. E. Rapp, *Microfluidics: Modeling, Mechanics and Mathematics* (Elsevier, New York, 2016), p. 283.
- [64] A. F. Mills, *Heat Transfer* (Prentice Hall, Englewood Cliffs, NJ, 1999).
- [65] A. Bejan, *Convection Heat Transfer* (John Wiley & Sons, New York, 2013).
- [66] R. Karwa, *Heat and Mass Transfer* (Springer, New York, 2020), p. 565.